

Performance of OFDM-FSO Communication System with Different Modulation Schemes over Gamma-Gamma Turbulence Channel

Bukola D. Ajewole¹, Kehinde O. Odeyemi², Pius A. Owolawi³, and Viranjay M. Srivastava¹

¹University of Kwazulu-Natal, Durban, 4001, South Africa

²University of Ibadan, 900001, Nigeria

³Tshwane University of technology, Pretoria, 0001, South Africa

Email: ajewolebukola561@yahoo.com

Abstract—Free Space Optical (FSO) has emerged as a commercially viable standalone wireless technology as well as complementary technology to Radio Frequency (RF) and millimeter wave wireless systems for reliable and rapid deployment for high-speed data, voice and video within the access networks. However, the atmospheric channel is affected by thick fog, smoke, and turbulence as well as the challenge to the attainment of 99.999% availability. These factors pose challenges to long-range terrestrial and Space FSO communication links. In this research, the performance of Orthogonal Frequency Division Multiplexing (OFDM) - Free Space Optical (FSO) communication system over Gamma-Gamma Turbulence channel is investigated. The performance of the system is impeded by various fluctuations of irradiance and atmospheric turbulence. The OFDM-FSO channel is adapted to alleviate the effect of channel impairments by employing two traditional modulation schemes namely: Binary Phase Shift Keying (BPSK) and M-ary Quadrature Amplitude Modulation (QAM). A comprehensive analysis of Average Bit Error Rate (ABER) versus Carrier to Noise plus Distortion Ratio (CNDP) have been carried out for the above modulation schemes. In addition, Forward Error Correction (FEC) has been added to the system to enhance the robustness of the chosen modulations to further reduce the effect of turbulence and scintillation on the FSO channel. The results obtained illustrates that the coded BPSK has a better error performance when compared to other modulation scheme used at all the considered turbulence thresholds.

Index Terms—Atmospheric turbulence, free space optical communication, Orthogonal Frequency Division Multiplexing (OFDM), Gamma-Gamma turbulence model, Binary Phase Shifting Keying (BPSK) modulation, Quadrature Amplitude Modulation (QAM).

I. INTRODUCTION

In recent years, a series of evolution and enormous improvements have been seen in communication and information technology industries. As a result of an increase in user demands and services such as high-speed internet, live-streaming, video-conferencing and etc., thus, an exponential increase in the need for bandwidth and channel capacity expansion to meet all demands are not negotiable. These have been brought about by the

increasing demand for higher data rate, higher efficiency, better Quality of Service (QoS), high-speed internet, live-streaming, video-conferencing and so on. These demands are required and desired by many users coupled with high cost of system installation and use of lower bandwidths have led to the congestion in the use of Radio Frequency (RF) spectrum at frequencies at the lower bands. The FSO systems are highly favored with high data rate and large capacity coverage as compared with RF which is limited by diffraction and scattering. Hence, poor receiver sensitivity [1], [2]. It is also very robust to blocking and shadowing and is therefore preferred for individual usage due to its coverage, mobility and versatility in indoor and outdoor environments [1]-[3].

FSO communication is a wireless system that uses the optical carrier in the transmission of information through free space (atmospheric channel). FSO communication is a technology that may stand on its own or serves as a complementary access technology to the RF systems, as it offers an efficient solution for last mile connectivity, it offers a number of unique advantages over RF. Some of the advantages are: it has an abundance of unregulated bandwidth thus, making the transmission possible at a very high speed (up to 2.5 Gbps of data throughput). Unlike the RF, it is a highly secured connectivity as the laser beam cannot be detected with spectrum analyzer thereby making interception of the transmitted data impossible. Installation of FSO is relatively inexpensive and less tasking as the transmission is through free space. Thus, making it readily accessible with no spectrum utilization tariffs (licensing) required as contrary to that of RF. The power consumption in FSO is lower than that of RF and, it has minimal absorption effect at 800-890 nm and 1550 nm [4]-[8]. In spite of the numerous advantages of FSO, and because the medium of transmission is air as light passes through it, some environmental challenges which are inevitable affects its performance. A major limitation in FSO is atmospheric turbulence which occurs as a result of weather properties (such as rain, haze, fog, and snow) which then resulted to FSO's signal attenuation losses and random fluctuation of the received signal due to variation in temperature and

pressure [9], [10]. Other drawbacks of FSO include physical obstruction that appears in the Line of Sight (LOS) of transmission due to blocking and/ or shadowing. Scintillation is also considered to be a limitation in FSO as temperature variation from the earth or artificial devices cause fluctuations in the amplitude of the signal [11].

Various channel distribution techniques such as Gamma-Gamma, Log-Normal, Negative Exponential, K-Distribution have been introduced to describe and model the various impacts of atmospheric turbulence on FSO fading channel [1], [12]. In this research work, authors have considered the Gamma-Gamma channel distribution as the most suitable distribution due to inherent characteristics to describe and model the weak to strong turbulence for the FSO channel [1], [13]. Binary Phase Shift Keying (BPSK) and Quadrature Amplitude Modulation (M-ary QAM), have been proposed as the modulation schemes to be used over the FSO's system. As BPSK and M-QAM require no adaptive threshold schemes, therefore they offer better performances when compared to other modulation schemes under the same atmospheric turbulence thresholds.

However, the system performance of FSO can be enhanced by introducing the Orthogonal Frequency Division Multiplexing (OFDM) scheme into the system. OFDM is a modulation technique used in wireless communication systems. It is an effective solution to address the Inter-Symbol Interference (ISI) caused by a dispersive channel and robust to frequency selective fading [11], [14]. The basic principle of OFDM is to split a high-rate data stream into a number of lower rate streams that are being transmitted simultaneously over sub-carriers. It is applied to FSO due to its high bandwidth efficiency, increased tolerance capacity against frequency selective fading and narrow-band. The combined OFDM based FSO signal is propagated through the atmospheric turbulent channel, scintillation which resulted in the aberration effects. This process results in a change in the amplitude and phase respectively of the OFDM based FSO [3].

The Forward Error Correction (FEC) technique performs a significant role in the enhancement of the performance of OFDM-FSO. It introduces redundancy and frequency diversity to the system, with the aim of overcoming signal degradation. Which causes fading in the FSO's atmospheric channel and the improvement attribute is termed as channel coding. In channel coding, information is mapped to ensure suitable data is transmitted over a channel by adding extra bits with information by the encoder while the decoder extracts the errors present in the transmitted information at the receiver of the channel [15]. In ref. [16], OFDM was transmitted over Rayleigh, Rician, and Nakagami fading channel. The BER performance was investigated and examined. In ref. [17], the performance of 16-QAM in OFDM-FSO communication was analyzed over gamma-gamma channel. However, ref. [16] did not consider

OFDM over FSO and the BER performance was just examined over AWGN, while ref. [17], did not include the investigation of the other higher modulation schemes in order to examine the performance of the system. A basic schematic diagram of OFDM-FSO system is shown in Fig. 1.

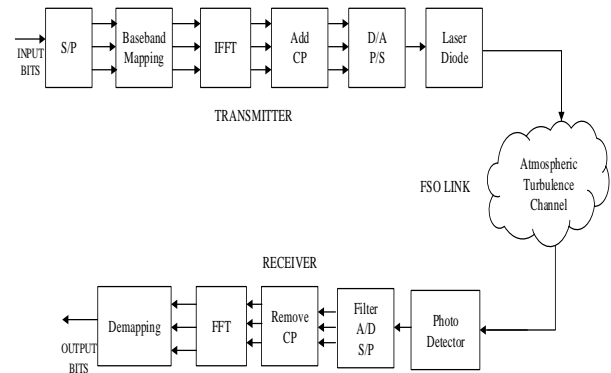


Fig. 1. The schematic diagram of OFDM-FSO system.

In this paper, authors have proposed a model to describe the ABER performance of BPSK and M-QAM and coded BPSK and M-QAM over the gamma-gamma turbulence channel and examined under different weather conditions. Also, the effect of atmospheric turbulence on the link distance between the transmitter and the receiver is also being investigated. Furthermore, the convolutional code is being employed to improve the overall error performance in the system. This paper has been organized as follows. Section II described the proposed OFDM-FSO system model. Atmospheric turbulence channel is discussed in section III. Section IV have the mathematical analysis of the ABER performance of BPSK and M-ary QAM in OFDM-FSO over Gamma-Gamma channel, Section V shows the simulated results using the Matlab software. Finally, the Section VI concludes the work and recommend the future aspects.

II. PROPOSED OFDM-FSO SYSTEM MODEL

The Orthogonal Frequency Division Multiplexing (OFDM) is a method of encoding digital data on multiple carrier frequencies. It can also be described as multicarrier modulation schemes, in which high-rate data-stream is split into a number of lower rate streams and are being transmitted simultaneously over a number of subcarrier or several narrowband channels at different frequencies. The Inverse Fourier Transform (IFFT) block is the main component of the transmitter and while its counterpart is the Fast Fourier Transform (FFT) which is situated in the receiver. The input in IFFT is a complex vector $X_m = [X_0 X_1 X_2 \dots X_{N-1}]$, where N represent the size of the IFFT and X_m represents the transmit signals from the IFFT [11]. The general expression for a transmitted signal over a channel is expressed as [11]:

$$X_j = \frac{1}{\sqrt{N}} \sum_{k=0}^{N-1} X_m \exp\left(\frac{j2\pi km}{N}\right) \text{ for } 0 \leq k \leq N-1 \quad (1)$$

where X_j is the transmitted signal over the channel after the cyclic prefix has been added and ISI is eliminated. N represents the size of the IFFT, m is the IFFT input at the transmit antenna and k is the OFDM symbol at the transmit antenna after the IFFT. The OFDM system just before the Laser Diode (LD) of the transmitter is given as [18]:

$$S_{ofdm}(t) = \sum_{j=0}^{N-1} S_j(t) \quad (2)$$

$$= \sum_{j=0}^{N-1} X_j \exp \left[2\pi i \left(\frac{n}{T_s} + f_c \right) t \right] \quad (3)$$

where w_n is the frequency for each OFDM, N represents a total number of the subcarriers, f_c denotes the carrier frequency, T_s represents the OFDM duration symbol and X_j^i represent the complex data symbol of the $j^{i\text{th}}$. The transmitted optical power $P(t)$ is expressed as [17], [18]

$$P_t(t) = P_o \left[1 + \sum_{j=0}^{N-1} m_{j_i} S_{j_i}(t) + \alpha_3 \left(\sum_{j=0}^{N-1} m_{j_i} S_{j_i}(t) \right)^3 \right] \quad (4)$$

where p_o , m_{j_i} and α_3 are the average transmitted optical power, optical modulation index (OMI) for each OFDM subcarrier and the third-order non-linear coefficient [14], [19]. The received power after the optical OFDM signal has been propagated through the FSO system is given as [19]:

$$P_r(t) = P_t(t) L_{tot} + n(t) \quad (5)$$

where L_{tot} is the total losses of the optical signal which is occurred as a result of the FSO experienced the atmospheric turbulence and n is the Additive White Gaussian Noise (AWGN) [19]. A major limiting factor for the performance of the system is the Inter-Modulation Distortion (IMD) which occurs when two or more signals are combined in an active system, thereby generating a new signal which is most likely to fall into another frequency band of the system. However, it becomes significant in this system due to the LD nonlinear responsivity [18], [19]. The carrier to noise of the system plus the distortion for each OFDM subcarrier is given as [20]:

$$CNDR_j(I) = \frac{(M_{j_i} \rho L_{tot} P_t I)^2}{2 \left(\frac{N_0}{T_s} + \sigma_{j,IMD}^2 \right)} \quad (6)$$

The instantaneous and average CNDR for each OFDM subcarrier is expressed as:

$$CNDR_j(I) \approx \frac{M^2_{j_i} \rho^2 L^2_{tot} P^2_t I^2}{2 \left(\left(\frac{N_0}{T_s} \right)_{AV} + \left(\sigma_{j,IMD}^2 \right)_{AV} \right)} \quad (7)$$

AV , ρ , T , δ and F are the average over scintillation value, PD responsivity, temperature, electron charge and noise present in the receiver, respectively. The $N_0 = \frac{4K_B T F}{R_L} + 2\delta l_0 + l^2_0 (RIN)$, where K_B , l_0 and R_L are the Boltzmann's constant, received photocurrent and resistor load, respectively. IMD and RIN is the inter-modulation distortion and is the relative intensity noise. [19], [21].

III. ATMOSPHERIC TURBULENCE CHANNEL

Atmospheric turbulence can reduce the performance of FSO link, especially over a distance of 1 km or longer. The atmospheric turbulence is modeled by gamma-gamma distribution. It is based on the modulation technique where fluctuation of light radiation traversing a turbulent atmosphere is assumed to consist of scattering and refraction effects [1]. It describes a wide range of turbulence condition from weak to strong. The Gamma-Gamma Probability Density Function (PDF) is given by [13]:

$$F_h(h) = \frac{2(\alpha\beta)^{\frac{\alpha+\beta}{2}}}{\Gamma(\alpha)\Gamma(\beta)} h^{\frac{\alpha+\beta}{2}} K_{\alpha-\beta} \left(2\sqrt{\alpha\beta}h \right), h > 0 \quad (8)$$

where $K_{\alpha-\beta}$ is the modified Bessel function of the second kind of order $\alpha-\beta$. The α_t and β_t are the effective numbers of small scale and large scale eddies of the scattering environment and $\Gamma(\cdot)$ is the gamma function, h is the irradiance also referred to as path loss. The parameters α_t and β_t represent the effective number of large-scale cells of the scattering process and the effective number of small-scale cells respectively [1], [22], [23].

$$\alpha = \left(\exp \left(\frac{0.49\sigma_i^2}{(1+1.1\sigma_i^{12/5})^{7/6}} \right) - 1 \right)^{-1} \quad (9)$$

$$\beta = \left(\exp \left(\frac{0.51\sigma_i^2}{(1+0.69\sigma_i^{12/5})^{7/6}} \right) - 1 \right)^{-1} \quad (10)$$

where $\sigma_i^2 = 0.5 C_n^2 K^{7/6} L^{11/6}$ is Rytov variance, $k = \left(2\pi/\lambda \right)$, where λ is the optical wavelength, L is the link distance between the transmitter and receiver and C_n^2 ($m^{-2/3}$) is the scintillation index [1], [13].

IV. PERFORMANCE ANALYSIS

A. Average Bit Error Rate (ABER)

The Average Bit Error Rate (ABER) performance of the OFDM-FSO optical signal in the Gamma-Gamma (GG) turbulence channel for BPSK and M-QAM modulation is analyzed in this section. The degree to which the atmospheric turbulence presents in the FSO

link has degraded the transmitted OFDM signal and this may be estimated by calculating the Bit Error Rate (BER) probability. The PDF of Gamma-Gamma channel presents in FSO link is given in Eq. (8). By expressing the Bessel function in terms of Meijer G function [24], Eq. (8) may be re-written as:

$$F_h(h) = \frac{(\alpha\beta)^{\frac{(\alpha+\beta)}{2}} h^{\frac{(\alpha+\beta)}{2}-1}}{\Gamma(\alpha)\Gamma(\beta)h_a^{\frac{(\alpha+\beta)}{2}}} G_{0,2}^{2,0} \left(\frac{\alpha\beta h}{h_a} \middle| \begin{matrix} - \\ \frac{(\alpha+\beta)}{2}, \frac{(\beta-\alpha)}{2} \end{matrix} \right) \quad (11)$$

where h_a is the atmospheric attenuation and h is the channel state. The ABER of OFDM-FSO over Gamma-Gamma channel is given as [25],[26]:

$$ABER = \int_0^{\infty} P_e(h) F_h(h) dh \quad (12)$$

The average BER for the BPSK- OFDM signal may be approximated as [24]:

$$P_e(h) = \frac{N^{-1}}{\log_a(2)} \sum_{j=0}^{N-1} \text{erfc} \left(\sqrt{CND R_j(h)} \sin\left(\frac{\pi}{2}\right) \right) \quad (13)$$

Therefore, by substituting BPSK Eq. (13) into Eq. (12), the ABER becomes

$$\frac{N^{-1}}{\log_a(2)} \sum_{j=0}^{N-1} \int_0^{\infty} \text{erfc} \left(\sqrt{CND R_j(h)} \sin\left(\frac{\pi}{2}\right) \right) F_h(h) dh \quad (14)$$

Then, substituting $F_h(h)$ in Eq. (11) into Eq. (14), we have the expression

$$\begin{aligned} & \frac{(\alpha\beta)^{\frac{(\alpha+\beta)}{2}}}{N \log_2(2) \Gamma(\alpha) \Gamma(\beta) h_a^{\frac{(\alpha+\beta)}{2}}} \sum_{j=0}^{N-1} \int_0^{\infty} h^{\frac{(\alpha+\beta)}{2}-1} \text{erfc}(\sqrt{CND R_j(h)}) \sin\left(\frac{\pi}{2}\right) \\ & \times G_{0,2}^{2,0} \left(\frac{\alpha\beta h}{h_a} \middle| \begin{matrix} - \\ \frac{\alpha-\beta}{2}, \frac{\beta-\alpha}{2} \end{matrix} \right) dh \end{aligned} \quad (15)$$

The complementary error function erfc may be written in terms of Meijer G function as [27], [28]:

$$\text{erfc}(x) = \frac{1}{\sqrt{\pi}} G_{1,2}^{2,0} \left(x \middle| \begin{matrix} - \\ 0, \frac{1}{2} \end{matrix} \right) \quad (16)$$

where

$$x = CND R_j(h) \times \left(\sin\left(\frac{\pi}{2}\right) \right) \quad (17)$$

The average bit error rate (ABER) for OFDM-FSO link on BPSK modulation scheme may be written as [28]:

$$\begin{aligned} ABER &= \frac{(\alpha\beta)^{\frac{(\alpha+\beta)}{2}}}{\sqrt{\pi} N \log_2(2) \Gamma(\alpha) \Gamma(\beta) h_a^{\frac{(\alpha+\beta)}{2}}} \sum_{j=0}^{N-1} \int_0^{\infty} h^{\frac{(\alpha+\beta)}{2}-1} \times \\ & G_{0,2}^{2,0} \left(\frac{\alpha\beta h}{h_a} \middle| \begin{matrix} - \\ \frac{\alpha-\beta}{2}, \frac{\beta-\alpha}{2} \end{matrix} \right) G_{1,2}^{2,0} \left(\frac{h^2}{2} \middle| \begin{matrix} 1 \\ 0, \frac{1}{2} \end{matrix} \right) dh \end{aligned} \quad (18)$$

The ABER for uncoded BPSK OFDM-FSO can be solved by applying the integral identity given in [29]:

$$\begin{aligned} &= \frac{2^{\alpha+\beta}}{N \log_2(2) \Gamma(\alpha) \Gamma(\beta) 4\pi^{\frac{3}{4}}} \sum_{j=0}^{N-1} G_{5,2}^{2,4} \\ & \left(\frac{8xh_a^2}{(\alpha\beta)^2} \middle| \begin{matrix} 1-\alpha, \frac{2-\alpha}{2}, \frac{1-\beta}{2}, \frac{2-\beta}{2} \\ 0, \frac{1}{2} \end{matrix} \right) \end{aligned} \quad (19)$$

Similarly, the average bit error rate (ABER) for OFDM-FSO link on M-QAM modulation can be expressed as [24], [25], by substituting BER for M-QAM into Eq. (12), then new expression ABER is given:

$$\frac{2}{\log_2(M)} \sum_{j=0}^{N-1} \int_0^{\infty} \left[1 - \frac{1}{\sqrt{M}} \right] \text{erfc} \left(\sqrt{\frac{3 \log_2(M)}{M-1}} \times \frac{CND R_j(h) h^2}{2} \right) F_h(h) dh \quad (20)$$

By substituting Eq. (20) into Eq. (12) and expressing in Meijer G function

$$\begin{aligned} & \equiv \frac{2^{\alpha+\beta}}{\log_2(M) \Gamma(\alpha) \Gamma(\beta)} \left[1 - \frac{1}{\sqrt{M}} \right] \sum_{j=0}^{N-1} \int_0^{\infty} \text{erfc} \left(\sqrt{\frac{3 \log_2(M)}{M-1}} \frac{CND R_j(h) h^2}{2} \right) \\ & \times G_{0,2}^{2,0} \left(\frac{\alpha\beta h}{h_a} \middle| \begin{matrix} - \\ \frac{\alpha-\beta}{2}, \frac{\beta-\alpha}{2} \end{matrix} \right) dh \end{aligned} \quad (21)$$

Converting the erfc equation to Meijer G function and by evaluating the integral identity given in [29] then, the ABER for received uncoded M-QAM signal may be re-written as:

$$\begin{aligned} & \equiv \frac{2^{\alpha+\beta}}{\log_2(M) \Gamma(\alpha) \Gamma(\beta) \pi^{\frac{3}{4}}} \left[1 - \frac{1}{\sqrt{M}} \right] G_{5,2}^{2,4} \\ & \left[\frac{3 \log_2(M) h_a^2 8 CND R_j(h)}{(M-1) (\alpha\beta)^2} \middle| \begin{matrix} 1-\alpha, \frac{\alpha-1}{2}, \frac{1-\beta}{2}, \frac{2-\beta}{2} \\ 0, \frac{1}{2} \end{matrix} \right] \end{aligned} \quad (22)$$

B. Convolutional Coding (Hard Coding)

The performance of the uncoded BPSK and M-QAM can be further improved by adding a convolutional encoder and decoder to the system. The input data stream is encoded first by the convolutional encoder, the encoded data-streams is then interleaved by a random interleaver and then input into the BPSK and M-QAM modulators. The outputs of BPSK and M-QAM demodulators are deinterleaved at the receiver side, the estimated information is then obtained by using the hard decision Viterbi decoder. The average bit error rate for convolutional coded BPSK system assuming a perfect interleaving is written as [30]:

$$ABER_{CODED} \leq \sum_{x=d_{FREE}}^{\infty} \frac{1}{K} W_x B_x \quad (23)$$

where

$$B_x = \begin{cases} \sum_{e=\frac{x+1}{2}}^x \frac{x! P^e (1-p)^{x-e}}{e! (x-e)!} & , x \text{ odd} \\ \frac{x! P^{\frac{x}{2}} (1-p)^{\frac{x}{2}}}{2^{\frac{x}{2}} \left(x - \frac{x}{2} \right)!} + \sum_{e=\frac{x}{2}+1}^x \frac{x! P^e (1-p)^{x-e}}{e! (x-e)!} & , x \text{ even} \end{cases} \quad (24)$$

where d and d_{free} are the hamming distance and the minimum rate free distance of the convolutional code, W_x and B_x are the weighting coefficient and the binary symmetric channel, respectively.

V. SIMULATION RESULTS AND DISCUSSIONS

In this section, authors have presented results using suitable graphs in order to discuss the parameters affecting the performance of OFDM-FSO system as mathematically obtained in the previous section. The bit error rate probability for the two main modulation schemes used, BPSK and 64-QAM are derived analytically. The FSO link is modeled using the Gamma-Gamma turbulence distribution with the values of α and β obtained using Eq. (8) and Eq. (10) $\alpha = 2.902$, $\beta = 2.510$ for weak, $\alpha = 2.296$, $\beta = 1.822$ for moderate, and $\alpha = 2.064$, $\beta = 1.342$ for strong turbulence conditions, the analysed link distance $L = 500$ m to 200 m. Throughout this study, the performance of OFDM-FSO was improved by using the convolutional code as the error correcting scheme.

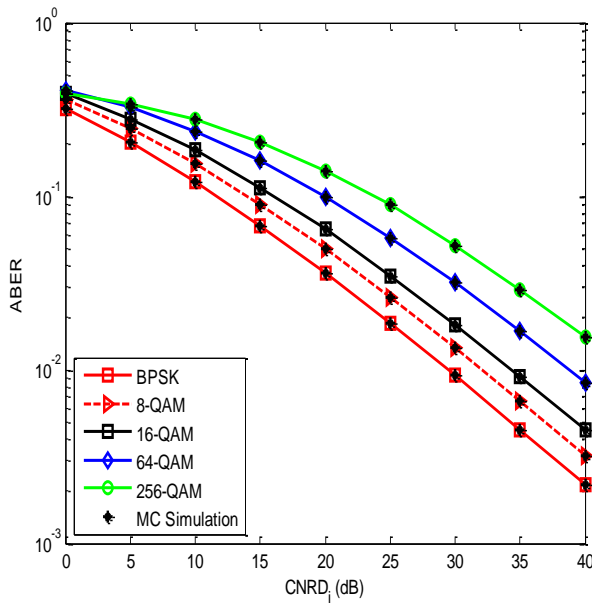


Fig. 2 performance comparison between BPSK and M-QAM uncoded system under strong turbulence.

Fig. 2 illustrates the ABER performance of uncoded BPSK and M-QAM OFDM-FSO link, for $M = 8, 16, 64, 256$, respectively under strong turbulence. As the modulation order M increases the error performance of the system becomes worse with an increase in turbulence from weak to a strong level. It can be seen that BPSK has a better performance with ABER of $\sim 10^{-3}$ while 256-QAM gives a worse performance with an error rate of $\sim 10^{-2}$.

In Fig. 3, authors have analyzed the performance of BPSK and 64-QAM OFDM-FSO system under the different turbulence conditions. It was also noticed that BPSK performed better in all turbulence conditions when compared to 64-QAM. It can be seen that the error performance and distortion worsen with an increase in the

modulation order, therefore, it has been observed that at weak turbulence BPSK requires a lower CNRD as compared to that of 64-QAM similarly.

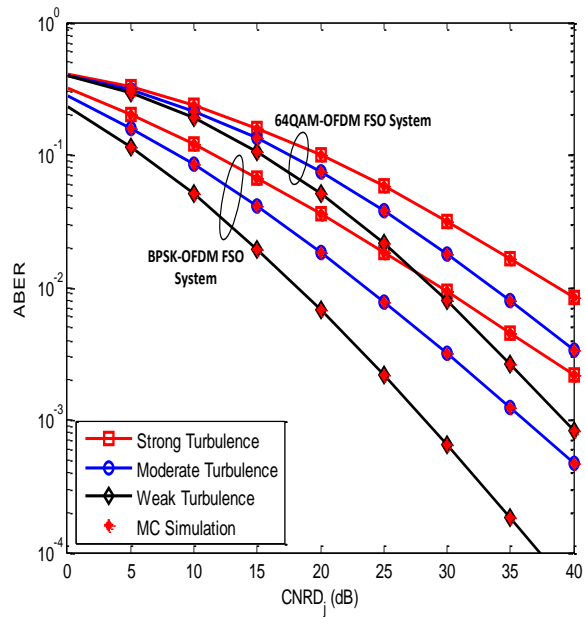


Fig. 3. Performance comparison between uncoded BPSK and 64-QAM OFDM-FSO system under different conditions.

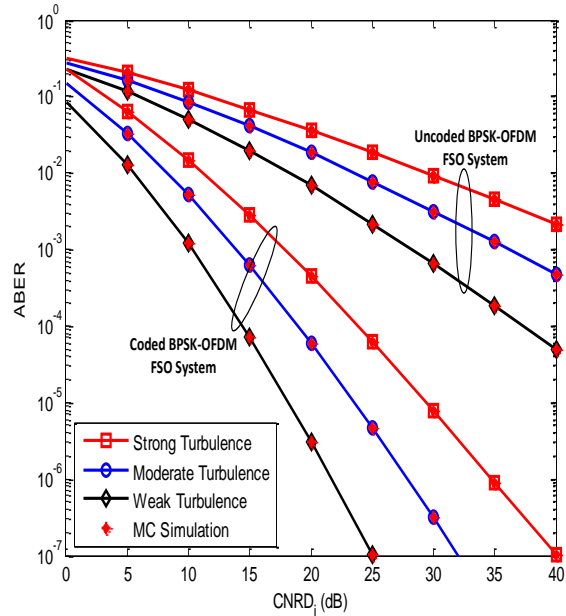


Fig. 4. Performance of uncoded BPSK OFDM-FSO system under different turbulence conditions.

Fig. 4 compares the performance between uncoded and coded BPSK –OFDM system over the three turbulence conditions. It can be seen that the ABER for uncoded BPSK was reduced from $10^{-2}, 10^{-3}, 10^{-4}$ to 10^{-7} respectively as the convolutional code was employed to the system. Similarly, the CNRD was also reduced, hereby giving a coding gain of 15dB and 8dB at weak and moderate turbulence regime.

The ABER performance of coded and uncoded BPSK and 64-QAM are compared in Fig. 5. The uncoded BPSK

and 64-QAM have a poor performance in the system due to degradation which occurs under the strong turbulence condition. The performance is improved by employing the coding technique, hence the coded BPSK achieved a better performance than the coded 64-QAM with a reduced ABER and CNRD. A coding gain of 16 dB was achieved for the coded BPSK.

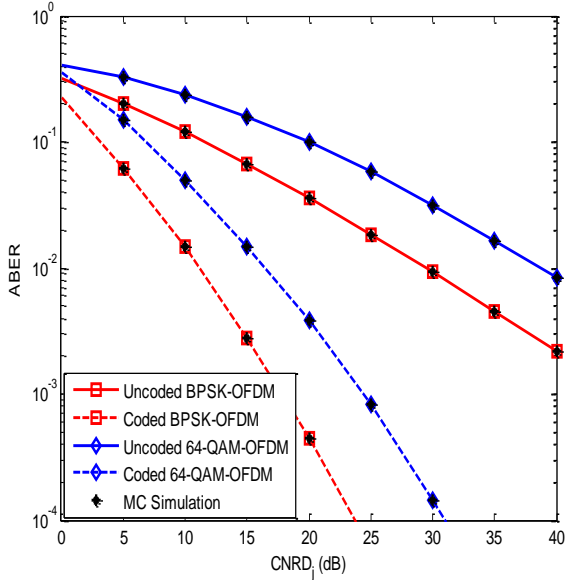


Fig. 5. Performance comparison between the coded and uncoded BPSK and 64-QAM OFDM-FSO system under strong turbulence condition.

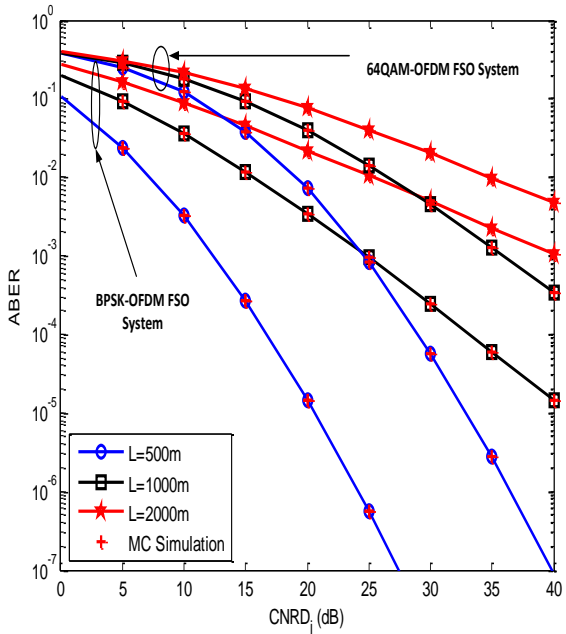


Fig. 6. Performance comparison between uncoded BPSK and 64-QAM OFDM-FSO system under different link distance.

The performance comparison between uncoded BPSK and 64-QAM OFDM FSO system under difference link distance is presented in Fig. 6. The best performance obtained has been recorded at the link distance of 500 m when the system has a low ABER of 10^{-7} while it has a worse performance at 2000 m at $\sim 10^{-2}$. In this figure, it may be deduced that as the distance between the

transmitter and the receiver increases, the error performance of the system increases respectively.

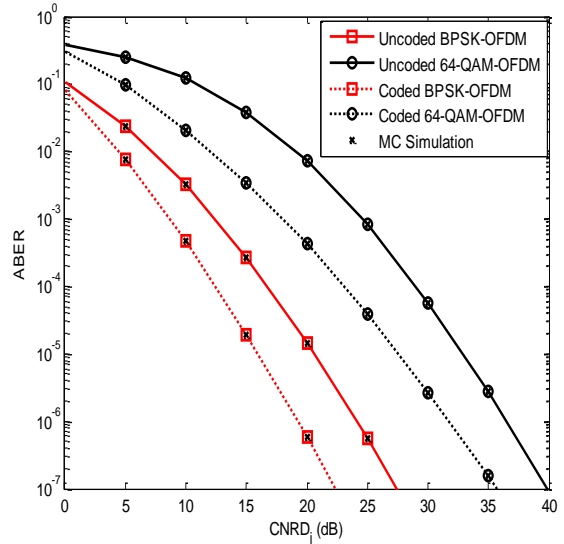


Fig. 7. Performance comparison between coded and uncoded BPSK and 64-QAM OFDM-FSO system at link distance of 500 m.

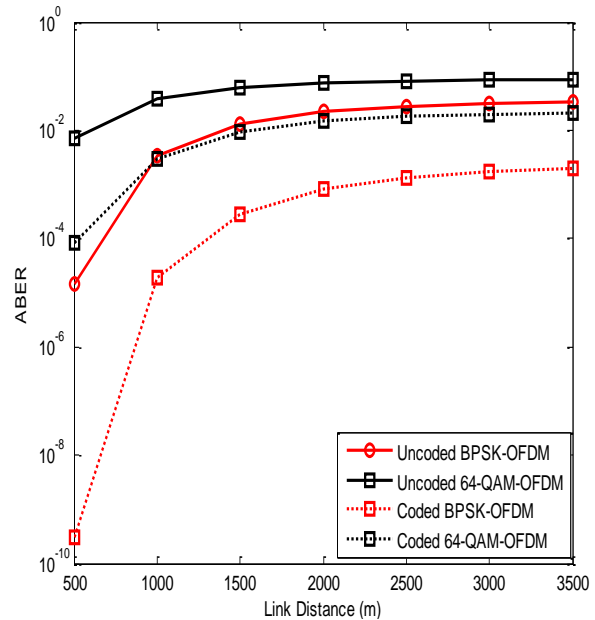


Fig. 8. Error performance vs link distance for coded and uncoded BPSK and 64-QAM OFDM-FSO system at CNRD = 20 dB.

The performance of coded and uncoded BPSK and 64-QAM OFDM-FSO system at 500 m is being compared in Fig. 7. It is observed that the distortion level has dropped due to the integrated coding with the modulation schemes of BPSK and 64-QAM, thus a positive coding gain of approximately 4dB was achieved for each transmitted data. Fig. 8 shows the error performance of coded and uncoded BPSK and 64-QAM over link distance at CNRD of 20dB. It is observed that all the modulation schemes used are feasible from 500 m to 3500 m at CNRD 20 dB. However, best performance for the system was recorded at 500 m, it is clearly shown that the system performance deteriorates with an increase in link distance. The ABER for both uncoded and coded 64-QAM is relatively high

due to its poor performance across all the distance with its worst at 3500 m with ABER of 10^{-2} and 10^{-4} . At 500 m the coded BPSK offers a better ABER performance of 10^{-10} than the uncoded BPSK with $\sim 10^{-5}$. However, it is evident that at the link distance of 3500 m, the system error performance is high irrespective of the modulation schemes used.

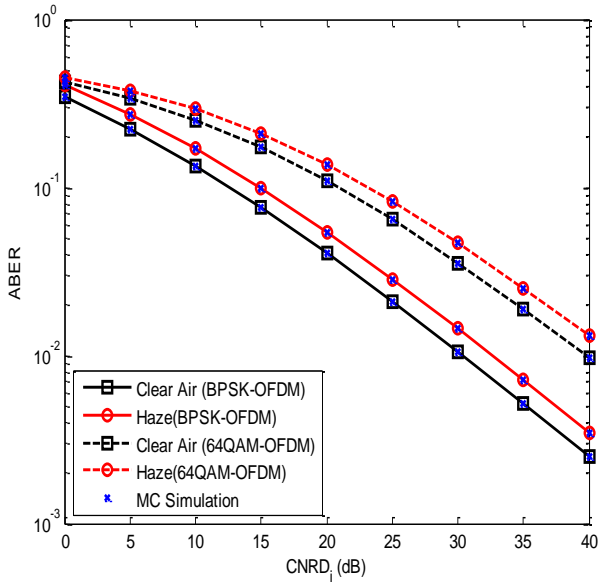


Fig. 9. Performance comparison between uncoded BPSK and 64-QAM OFDM-FSO system under different weather conditions.

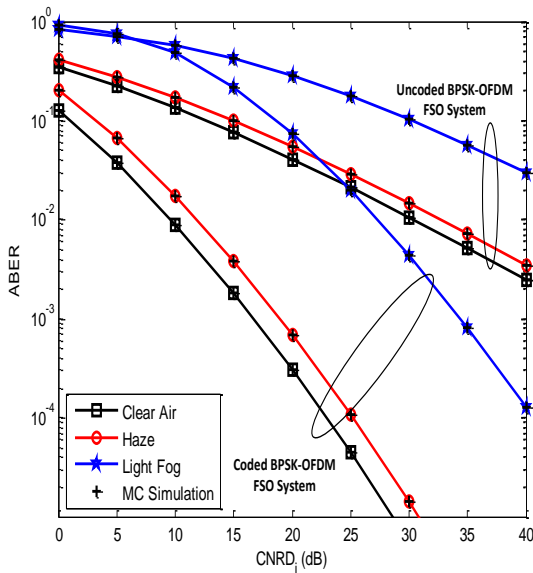


Fig. 10. Error performance of coded and uncoded BPSK OFDM-FSO systems under different weather conditions.

The performance of uncoded BPSK and 64-QAM FSO system are compared under different weather conditions in Fig. 9. In this case, two weather conditions (clear-air, haze) are investigated. It can be seen that BPSK offers a better system performance in clear-air and haze than 64-QAM. It is therefore shown that BPSK-OFDM has a degree of robustness against the variations of scattering and absorption present in the system.

The error performance of the coded and uncoded BPSK OFDM system under light fog, haze and clear-air are presented in figure 10. It is clearly shown that the uncoded BPSK has a poor performance under the three weather conditions investigated, while the worst performance is seen under the light fog. The effect of the convolutional coding technique is seen as it enhances the system performance by reducing the measure of error and CNRD present in the system. It is visible that the coded BPSK offers a better ABER performance than the uncoded BPSK in the system.

VI. CONCLUSIONS AND FUTURE ASPECTS

The mathematical analysis for the average bit error rate of BPSK and M-QAM OFDM-FSO links over the Gamma-Gamma turbulence channel have been derived in this paper. Using the derived expressions, we are able to analyze the effect of atmospheric turbulence and distortion over the modulation parameters of BPSK and M-QAM. The simulated results analysis show that BPSK offers a better performance against atmospheric turbulence when compared to M-QAM. It offers a lower error performance at all three turbulence regimes.

Furthermore, the performance of the OFDM-FSO system is also enhanced by employing the convolutional coding technique and the coded BPSK provides a better performance of approximately 20% over the uncoded BPSK in the system. The error performance of the system can be further improved in the future by employing other FEC techniques to the system.

REFERENCES

- [1] Z. Ghassemlooy, W. Popoola, and S. Rajbhandari, *Optical Wireless Communications System and Channel Modelling with MATLAB*, CRC Press, 2013, pp. 1-10.
- [2] S. Arnon, J. Barry, G. Karagiannidis, R. Schober, and M. Uysal, *Advanced Optical Wireless Communication*, Cambridge University Press, Cambridge, UK, 2012.
- [3] Institute of Electrical and Electronics Engineers, IEEE Standard 80211a-1999.
- [4] K. E. Wilson, "An overview of the GOLD experiment between the ETS-VI satellite and the table Mountain facility," 1996.
- [5] X. Zhu and J. M. Kahn, "Performance bounds for coded free-space optical communication through atmospheric turbulence channel," *IEEE Transactions Communications*, vol. 51, no. 8, pp. 1233-1239, 2003.
- [6] P. J. Titterton, "Power reduction and fluctuations caused by narrow laser beam motion in the far field," *Applied Optics*, vol. 12, no. 2, pp. 423-425, 1973.
- [7] T. Tolker-Nielsen and G. Oppenhauser, "In-orbit test result of an operational optical intersatellite link between ARTEMIS and SPOT4, SILEX," *Proc. SPIE Free Space Laser Communication Technologies XIV*, USA, vol. 4635, pp. 1-15, 2002.
- [8] A. R. Katsuyoshi, "2 Overview of the optical inter-orbit communications engineering test satellite (OICETS)

- project,” *Journal of the National Institute of Information and Communications Technology*, vol. 59, no. 1-2, pp. 5–12, 2012.
- [9] A. Mansor, R. Mesleh, and M. Abaza “New challenges in wireless and free space optical communications,” *Optics and Laser in Engineering*, vol. 89, pp. 95-108, 2017.
- [10] C. K. Datsikas, K. P. Peppas, N. C. Sagias, and G. S. Tombras, “Serial free-space optical relaying communications over gamma-gamma atmospheric turbulence channels,” *IEEE/OSA Journal of Optics Communications and Networking*, vol. 2, no. 8, pp. 576-586, 2010.
- [11] R. V. Nee and R. Prasad, *OFDM for Wireless Multimedia Communications*, Norwell, MA: Artech House, 2000.
- [12] L. C. Andrews and R. L. Phillips, *Laser Beam Propagation through Random Media*, 2nd Ed., Washington, SPIE Press, 2005.
- [13] W. O. Popoola and Z. Ghassemlogy, “BPSK subcarrier intensity modulated free space optical communication in atmospheric turbulence,” *Journal of Lightwave Technology*, vol. 27, no. 8, pp. 967–973, 2009.
- [14] J. Armstrong, “OFDM for optical communication,” *Journal of Lightwave Technology*, vol. 27, no. 3, pp. 189-204, 2009.
- [15] K. D. Rao, *Channel Coding Techniques for Wireless Communications*, Springer 2015
- [16] P. Rajasekhar and V. R. Raju, “BER performance of 1024 (BPSK, QPSK & QAM) using OFDM over Rayleigh, Rician and Nakagami fading channel,” *International Journal of Computer Application*, vol. 164, no. 7, 2017.
- [17] Y. Wang, D. Wang, and J. Ma, “On the performance of coherent OFDM system in free space optical communications,” *IEEE Photonics Journal*, vol. 7, no. 4, 2015.
- [18] H. Al-Raweshidy and S. Komaki, *Radio Over Fiber Technologies for Mobile Communication Networks*, 1st Ed., Artech House, Norwell, MA, pp. 65-102, 2002.
- [19] A. Bekkali, C. B. Naila, K. Kazaura, K. Wakamori, and M. Matsumoto, “Transmission analysis of OFDM-based wireless services over turbulent radio-on-FSO links modeled by Gamma–Gamma distribution,” *IEEE Photonics Journal*, vol. 2, no. 3, pp. 509–520, 2010.
- [20] H. E. Nistazakis, A. N. Stassinakis, S. Sinanovic, W. O. Popoola, and G. S. Tombras, “Performance of quadrature amplitude modulation orthogonal frequency division multiplexing-based free space optical links with non-linear clipping effect over gamma–gamma modelled turbulence channels,” *Optoelectronics, IET*, vol. 9, no. 5, pp. 269-274, 2015.
- [21] V. W. Chan, “Free-Space optical communications,” *Journal of Lightwave Technology*, vol. 24, no. 12, pp. 4750-4762, 2006.
- [22] M. A. Al-Habash, L. C. Andrews, and R. L. Phillips, “Mathematical model for the irradiance probability density function of a laser beam propagating through turbulent media,” *Optical Engineering*, vol. 40, no. 8, pp. 1554-1562, 2001.
- [23] M. Selvi and K. Murugesan, “Performance of OFDM based FSO communication systems using M-ary PSK modulation,” *International Journal of Computer Applications*, vol. 49, no. 7, pp. 41–45, 2012.
- [24] V. S. Adamchik and O. I. Marichev, “The algorithm for calculating integrals of hypergeometric type functions and its realization in reduce system,” in *Proc. International Symposium on Symbolic and Algebraic Computation*, ACM, USA, 1990, pp. 212–224.
- [25] P. Kaur, V. K. Jain, and S. Kar, “Performance analysis of FSO array receivers in presence of atmospheric turbulence,” *IEEE Photonics Technology Letters*, vol. 26, no. 12, pp. 1165–1168, 2014.
- [26] X. Song, F. Yang, and J. Cheng, “Subcarrier intensity modulated optical wireless communications in atmospheric turbulence with pointing errors,” *Journal of Optical Communications and Networking*, vol. 5, no. 4, pp. 349 – 358, 2013.
- [27] A. P. Prudnikov, Y. A. Brychkov, and O. I. Marichev, *Integrals and Series*, Gordon and Breach Science Publishers, New York, 1986.
- [28] W. Function Site, Meijer G Function URL <http://functions.wolfram.com/PDF/MeijerG.pdf>, 2009.
- [29] A. B. Prudnikov, Y. A. Brychov, and O. I. Marichev, *Integrals and Series*, vol. 4, 1999.
- [30] S. Lin and D. J. Costello, *Error Control Coding*, Pearson Education India, 2001.

Ajewole D. Bukola holds a Bachelor in Engineering degree in Electrical and Electronics Engineering at the Federal University of Technology, Akure, Nigeria. She is currently studying to obtain her Masters of Science degree at the University of KwaZulu-Natal, Durban, South Africa. Her research interest are in optical wireless communication, MIMO systems and OFDM.

Kehinde O. Odeyemi currently a lecturer at the department of Electrical and Electronics Engineering, University of Ibadan, Nigeria. He obtained PhD in Electrical and Electronics Engineering from the University of KwaZulu-Natal, Durban, South Africa. He has written several articles and his research interest are in antenna design, optical wireless communications, diversity combining techniques and MIMO systems.

Pius A. Owolawi is currently a professor at Tshwane University of Technology, Pretoria, South Africa. His research interests are in the modeling of radio wave propagation at high frequency, fiber optic communication, radio planning and optimization techniques and renewable energy. He has written several research articles and serves as a reviewer for many scientific journals.

Viranjay M. Srivastava is currently a professor in the Department of Electronics Engineering, University of KwaZulu-Natal, Durban, South Africa. He has more than 15 years of teaching and research experience. He is a senior member of IEEE and IEEE HKN, and author of more than 180 scientific contributions including books, chapters and International refereed journals.